New role for the (pro)renin receptor in T cell development

Geisberger S., Maschke U., Gebhardt M., Kleinewietfeld M., Manzel A., Linker R.A., Chidgey A., Dechend R., Nguyen G., Daumke O., Muller D.N., Wright M.D., Binger K.J.

Blood
2015 JUL 23 ; 126(4): 504-507
2015 JUN 10 (first published online: accepted manuscript)
doi: 10.1182/blood-2015-03-635292

Publisher: The American Society of Hematology

Brief Report

IMMUNOBIOLOGY

New role for the (pro)renin receptor in T-cell development

Sabrina Geisberger,[1,2] Ulrike Maschke,[1,2] Matthias Gebhardt,[1,2] Markus Kleinewietfeld,[3] Arndt Manzel,[4] Ralf A. Linker,[4] Ann Chidgey,[5] Ralf Dechend,[1,6] Genevieve Nguyen,[7] Oliver Daumke,[2,8] Dominik N. Muller,[1,2] Mark D. Wright,[9] and Katrina J. Binger[1,2]

[1]Experimental and Clinical Research Center, an institutional cooperation between the Charité Medical Faculty and the Max-Delbruck Center for Molecular Medicine, Berlin, Germany; [2]Max-Delbruck Center for Molecular Medicine, Berlin, Germany; [3]Faculty of Medicine, Dresden University of Technology, Dresden, Germany; [4]Department of Neurology, University of Erlangen, Erlangen, Germany; [5]Stem Cells and Immune Regeneration Laboratory, Department of Anatomy and Developmental Biology, Monash University, Clayton, Australia; [6]HELIOS-Klinikum Berlin, Berlin, Germany; [7]INSERM and College de France, Center for Interdisciplinary Research in Biology, Paris, France; [8]Institute for Chemistry and Biochemistry, Freie Universität Berlin, Berlin, Germany; and [9]Department of Immunology, Monash University, Prahran, Australia

Key Points

- PRR deletion in T cells drastically reduces the number of peripheral and thymic CD3$^+$ T cells.
- We identify multiple stages of thymocyte development that require PRR expression.

The (pro)renin receptor (PRR) was originally thought to be important for regulating blood pressure via the renin-angiotensin system. However, it is now emerging that PRR has instead a generic role in cellular development. Here, we have specifically deleted PRR from T cells. T-cell–specific PRR-knockout mice had a significant decrease in thymic cellularity, corresponding with a 100-fold decrease in the number of CD4$^+$ and CD8$^+$ thymocytes, and a large increase in double-negative (DN) precursors. Gene expression analysis on sorted DN3 thymocytes indicated that PRR-deficient thymocytes have perturbations in key cellular pathways essential at the DN3 stage, including transcription and translation. Further characterization of DN T-cell progenitors leads us to propose that PRR deletion affects thymocyte survival and development at multiple stages; from DN3 through to DN4, double-positive, and single-positive CD4 and CD8. Our study thus identifies a new role for PRR in T-cell development. (*Blood*. 2015;126(4):504-507)

Introduction

The (pro)renin receptor (PRR) was originally identified as a receptor for (pro)renin.[1] Its discovery led to an enormous amount of research in the cardiovascular field because of the involvement of (pro)renin in promoting hypertension under conditions of renin-angiotensin system hyperactivation.[2] However, subsequent transgenic animal models failed to show a causal link between PRR and hypertension.[2-5] Instead, it has emerged that PRR is essential for cellular development and homeostasis. PRR is ubiquitously expressed, and total knockout in mice is embryonic lethal.[6] Several PRR conditional knockout (cKO) models have been characterized, all with severe phenotypes: acute kidney injury with podocyte,[7,8] heart failure with cardiomyocyte,[9] and impaired eye and kidney development with retinal[10] and uteric bud[11] cKO.

Disturbances in many processes have been observed upon deletion of PRR.[5,12] These effects appear to be central to the molecular association of PRR with the vacuolar (V)- adenosine triphosphatase (ATPase), where it is proposed that PRR regulates V-ATPase activity.[13] Much insight into PRR function has come from developmental biology studies, which showed that the association of PRR with the V-ATPase is essential for canonical Wnt signaling,[13] an important developmental pathway. Further studies in *Drosophila melanogaster* identified that knockdown of PRR perturbs trafficking of Wnt signaling receptors.[14,15] The role of Wnt signaling in T-cell development has been controversial, with some studies showing a role[16] and others not.[17,18] As PRR is highly expressed in lymphocytes,[19] we hypothesized that deletion of PRR from T cells would have implications for T-cell development.

Study design

We bred *ATP6AP2*$^{flox/+}$ females with male mice expressing Cre recombinase under the *Lck* promoter (supplemental Figure 1; available on the *Blood* Web site). Male mice with PRR conditionally deleted from T cells (*ATP6AP2*$^{flox/y}$;*Lck*^{Cre}) are hereafter referred to as "cKO." Full methods are available online (see supplemental Methods).

Results and discussion

The cellularity of peripheral lymphoid organs and blood were analyzed by flow cytometry. In PRR cKO mice, a significant decrease in CD3$^+$ T cells was observed in all tissues, with no difference in the number of B, macrophage, or dendritic cells (Figure 1A; supplemental Figures 2-3).

Submitted March 23, 2015; accepted June 8, 2015. Prepublished online as *Blood* First Edition paper, June 10, 2015; DOI 10.1182/blood-2015-03-635292.

S.G. and U.M. contributed equally to this study.

M.D.W. and K.J.B. contributed equally to this study.

The online version of this article contains a data supplement.

The publication costs of this article were defrayed in part by page charge payment. Therefore, and solely to indicate this fact, this article is hereby marked "advertisement" in accordance with 18 USC section 1734.

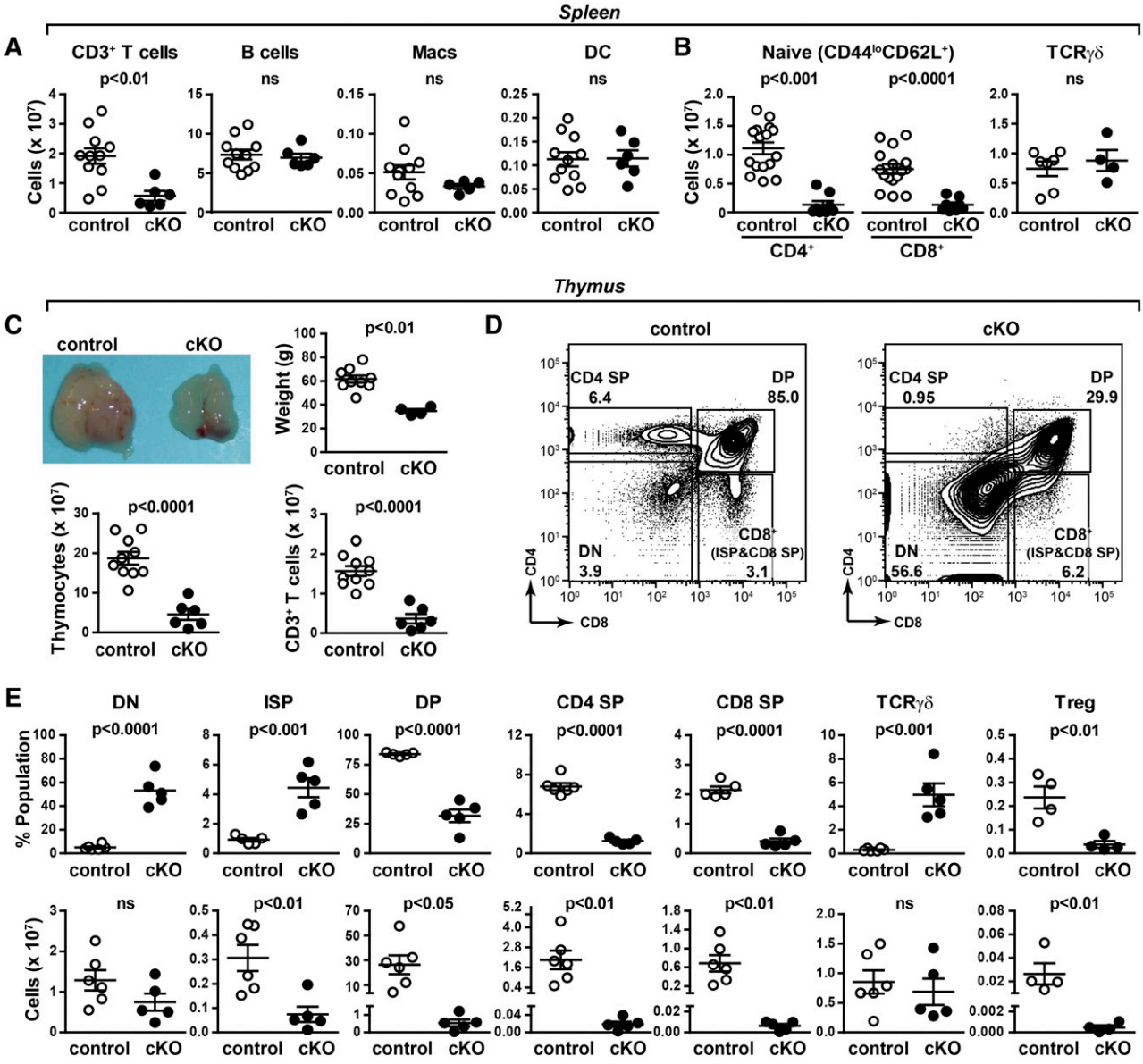

Figure 1. Abnormal thymic T-cell development in PRR cKO mice. (A) Absolute numbers of T (all $CD3^+$), B, macrophage, and dendritic cells from spleens of 7- to 8-week-old mice were determined by flow cytometry. (B) Absolute numbers of naïve ($CD44^{lo}CD62L^+$) $CD4^+$ and $CD8^+$ T cells and γδT cells. (C) Morphology, tissue weight, cellularity, and number of $CD3^+$ cells of thymi from 6-week-old mice. (D) Thymocytes from 6-week-old control and cKO mice were analyzed by flow cytometry. The gating strategy for CD4 and CD8 expression is shown. (E) From panel D: the percentage (top) and number (bottom) of DN, ISP, double-positive (DP), CD4 single-positive (SP), CD8 SP, TCRγδ, and regulatory T (Treg) cells.

A striking reduction in both $CD4^+$ and $CD8^+$ naïve T cells was evident, with no change in the number of peripheral T-cell receptor (TCR) γδ cells observed (Figure 1B). As PRR is found to be essential for homeostasis,[7-11] we asked if the remaining peripheral T cells had the PRR gene excised. We performed polymerase chain reaction (PCR) that specifically amplified a segment of the PRR gene only after it was mutated by Cre recombination (supplemental Figure 4). Using this approach, we could detect the recombined gene (ie, with the PRR gene excised) in thymic but not peripheral $CD90.2^+$ T cells, which expressed similar levels of PRR protein as control T cells (supplemental Figure 4). Together, these results indicate that peripheral cKO T cells simply do not develop or survive. Instead, those few cells that do not recombine the PRR gene have an enormous selective advantage and reach the periphery.

The striking reduction in peripheral naïve T cells is consistent with a defect in thymic T-cell development, so we turned our focus to this organ. A severe atrophy of PRR cKO thymi was observed, evidenced by a reduction in weight and cellularity (Figure 1C). PRR cKO thymi had a 10-fold increase in the proportion of double-negative (DN) thymocytes (Figure 1D). A significant increase in the proportion of intermediate single-positive (ISP) and TCRγδ cells was observed, whereas all other populations were decreased (Figure 1E). The number of DN cells was unchanged, whereas the numbers of ISP, DP, CD8 SP, CD4 SP, and regulatory T cells were reduced (Figure 1E). Histologic analysis indicated that the loss of SP T cells was associated with a reduction in the thymic medulla of cKO mice but preserved corticomedullary junction (supplemental Figure 5), consistent with other models of severe SP T-cell loss.[20] No change in the number of TCRγδ cells was evident. This is unsurprising as the lineage commitment for TCRγδ cells begins at the DN2 stage, prior to *Lck*-driven Cre recombinase expression.[16] Taken together, the almost 100-fold

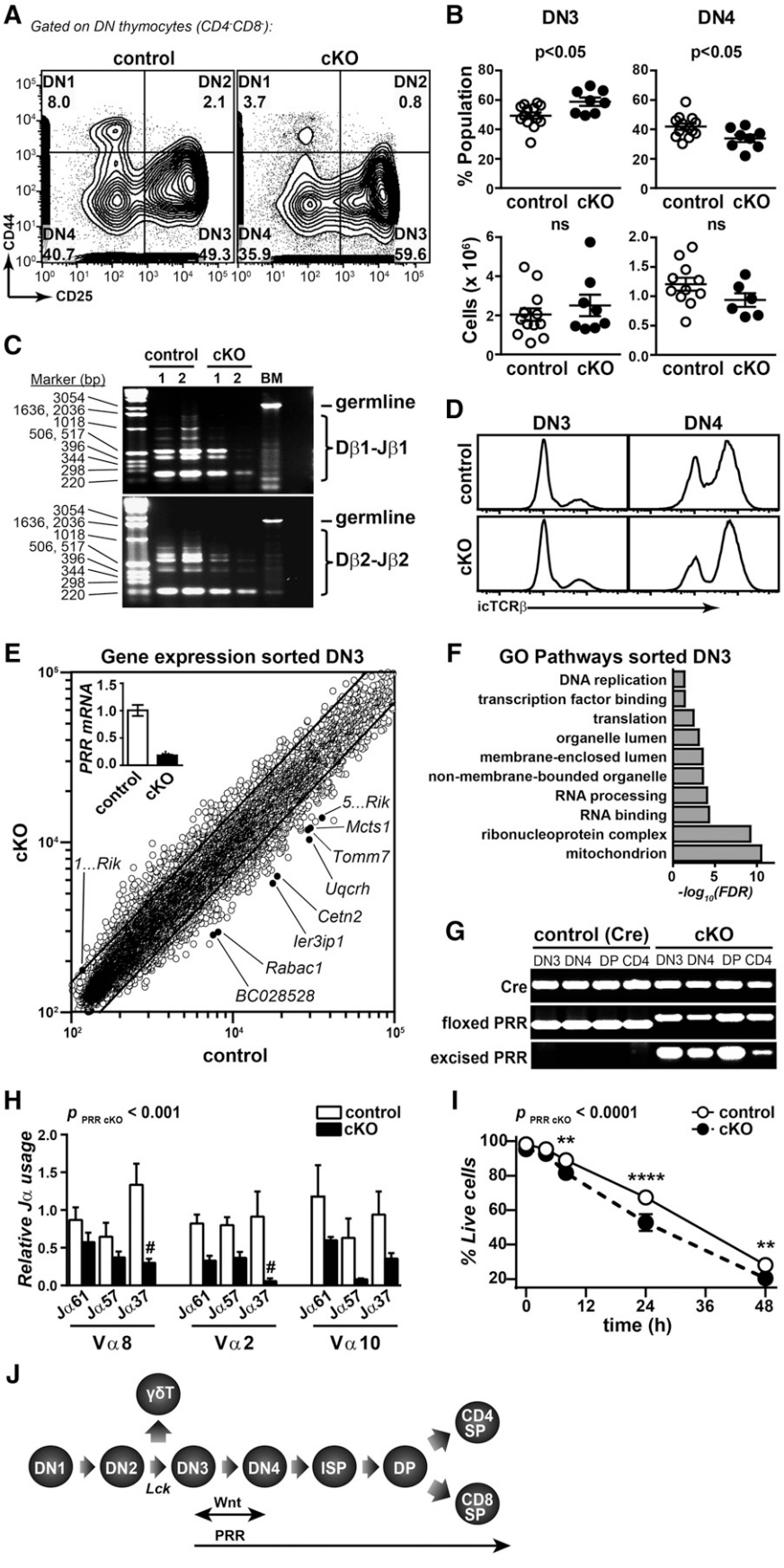

Figure 2. PRR cKO impairs thymocyte survival and development from DN3 and beyond. (A) Representative flow cytometry of CD25 and CD44 expression in DN ($CD4^-CD8^-$) thymocytes from 39-day-old mice. (B) The frequency and actual number of DN3 and DN4 cells from panel A. (C) TCRβ gene rearrangement by PCR of sorted DN4 cells from control and cKO mice. DNA from bone marrow (BM) cells is shown as a nonrearranged control. (D) Expression of intracellular TCRβ in DN3 and DN4 thymocytes as from panel B. (E) Scatter plot showing the comparison of gene expression from microarray analysis of DN3 sorted cells from control and cKO mice. Significantly different genes (by 1-way analysis of variance [ANOVA]; $q < 0.05$) are labeled (black circles). For clarity, the gene *5730437N04Rik* is abbreviated as "5…Rik," and the gene *1600029D21Rik* is abbreviated as "1…Rik." Inset shows PRR expression by real-time quantitative PCR. N = 3 biological replicates. (F) GO pathways that were significantly enriched in cKO DN3 cells (false-discovery rate [FDR] <0.5) are shown. Details of the genes in each pathway are listed in supplemental Table 1. (G) Representative PCR from sorted thymocytes from 39-day-old control and cKO mice to detect the unexcised PRR gene ("floxed") and mutated/deleted gene in cKO ("excised"). Cre recombinase expression is also shown. (H) TCRα gene rearrangement was determined in sorted DP cells from control and cKO mice by quantitative PCR with primers specific for Vα8, Vα2, and Vα10 in conjunction with different Jα primers. The *P* value shown for the effect of PRR deletion was calculated by 2-way ANOVA. #$P < .01$ by Sidak's multiple comparison test. N = 3-4. (I) Thymocytes from control and cKO mice were cultured in vitro with interleukin 7, and the proportion of live cells was determined by flow cytometry at the desired time points. The *P* value shown for the effect of PRR deletion was calculated by 2-way ANOVA. **$P < .01$; ****$P < .0001$ by Sidak's multiple comparison test. N = 5-9. (J) Schematic of T-cell development stages affected by PRR deletion.

reduction in SP cells indicates that PRR cKO mice have drastically altered thymocyte development.

We next analyzed early T-cell developmental events (DN1-4). There was an increase in the proportion of DN3 cells in cKO mice, which was correlated with a decreased proportion of DN4 (Figure 2A). These proportional changes were not associated with differences in the number of DN3 or DN4 (Figure 2B). At the DN3 stage, cells commit to the T-cell lineage and rearrange the TCR β-chain gene locus. PCR products corresponding to rearranged TCRβ locus were detected in both control and cKO cells, indicating that this process was not disturbed (Figure 2C). There was no difference in intracellular TCRβ levels (Figure 2D).

We next performed gene expression analysis of sorted DN3 cells (Figure 2E; supplemental Table 1A). In cKO, 615 and 518 genes were up- and downregulated >1.5-fold. Of these, 9 genes were significantly different and encoded molecules important for processes including the cell cycle (*Mcts1*, *Cetn2*), mitochondria (*Tomm7*, *Uqcrh*) and vesicular trafficking (*Ier3ip1*, *Rabac1*). We next performed gene ontology (GO) analysis on the differentially expressed genes (Figure 2F; supplemental Table 1B). Several GO pathways were enriched in cKO DN3 cells, indicating disturbances in transcription, translation, and the mitochondria. Collectively, these represent cellular activities essential for this developmental period, providing an explanation for why PRR deletion has such a profound effect on T-cell development.

Comparing our findings to conditional deletion of the Wnt pathway in T cells, several similarities are evident: reduction in peripheral T cells and a change in the proportion of DN3:DN4.[16] However, overall it is clear that PRR deletion induces a more profound phenotype. Wnt cKO led to an increase in the proportion of DN cells to 12%, and a partial block at the DN3-DN4 transition, leading to an increased number of DN3 cells and decreased DN4. In the periphery, there was a fourfold reduction in T cells, which did have the β-catenin deleted allele.[16] In contrast, PRR cKO leads to an increase in the proportion of DN cells to ~50% of thymocytes, we detect no increase in the number of DN3 cells, and we find that DN4 numbers are decreased only in old mice (data not shown). Furthermore, we are unable to detect the deleted allele in peripheral T cells, indicating that PRR-deficient T cells do not develop/survive. To understand these results further, we sorted thymocytes and again performed PCR to specifically identify cKO cells. This revealed the presence of cKO cells beyond the DN3 stage, including DN4, DP, and CD4 SP (Figure 2G). We analyzed DP cells further and observed an impaired survival and, subsequently, rearrangement of the TCR α chain (*Tcra*) (Figure 2H-I). Thus, given the striking severity of our phenotype, that no single precursor thymocyte population accumulates, and that we also observe defects in DP cells, we propose that deletion of PRR affects thymocyte survival and development from DN3 and beyond (Figure 2J).

Acknowledgments

The authors thank Jana Czychi, Ilona Kamer, Sabine Schmidt, and Dr Hans-Peter Rahn for technical assistance.

This work was supported by the National Health and Medical Research Council of Australia (K.J.B. and M.D.W.), and the German Research Foundation and German Center for Cardiovascular Research (D.N.M.).

Authorship

Contribution: S.G., U.M., M.G., A.M., and K.J.B. performed experiments; M.K., R.A.L., R.D., A.C., and O.D. gave advice; G.N. provided mice; and D.N.M., M.D.W., and K.J.B. designed and wrote the study.

Conflict-of-interest disclosure: The authors declare no competing financial interests.

Correspondence: Katrina J. Binger, Experimental and Clinical Research Center, Lindenbergerweg 80, Berlin, 13125, Germany; e-mail: katrinabinger@gmail.com; and Dominik N. Muller, Experimental and Clinical Research Center, Lindenbergerweg 80, Berlin, 13125, Germany; e-mail: dominik.mueller@mdc-berlin.de.

References

1. Nguyen G, Delarue F, Burcklé C, Bouzhir L, Giller T, Sraer JD. Pivotal role of the renin/prorenin receptor in angiotensin II production and cellular responses to renin. *J Clin Invest.* 2002;109(11):1417-1427.
2. Müller DN, Binger KJ, Riediger F. Prorenin receptor regulates more than the renin-angiotensin system. *Ann Med.* 2012;44(suppl 1):S43-S48.
3. Mahmud H, Candido WM, van Genne L, et al. Cardiac function and architecture are maintained in a model of cardiorestricted overexpression of the prorenin-renin receptor. *PLoS ONE.* 2014;9(2):e89929.
4. Rosendahl A, Niemann G, Lange S, et al. Increased expression of (pro)renin receptor does not cause hypertension or cardiac and renal fibrosis in mice. *Lab Invest.* 2014;94(8):863-872.
5. Batenburg WW, Danser AH. (Pro)renin and its receptors: pathophysiological implications. *Clin Sci (Lond).* 2012;123(3):121-133.
6. Burcklé C, Bader M. Prorenin and its ancient receptor. *Hypertension.* 2006;48(4):549-551.
7. Oshima Y, Kinouchi K, Ichihara A, et al. Prorenin receptor is essential for normal podocyte structure and function. *J Am Soc Nephrol.* 2011;22(12):2203-2212.
8. Riediger F, Quack I, Qadri F, et al. Prorenin receptor is essential for podocyte autophagy and survival. *J Am Soc Nephrol.* 2011;22(12):2193-2202.
9. Kinouchi K, Ichihara A, Sano M, et al. The (pro)renin receptor/ATP6AP2 is essential for vacuolar H+-ATPase assembly in murine cardiomyocytes. *Circ Res.* 2010;107(1):30-34.
10. Kanda A, Noda K, Yuki K, et al. Atp6ap2/(pro)renin receptor interacts with Par3 as a cell polarity determinant required for laminar formation during retinal development in mice. *J Neurosci.* 2013;33(49):19341-19351.
11. Song R, Preston G, Ichihara A, Yosypiv IV. Deletion of the prorenin receptor from the ureteric bud causes renal hypodysplasia. *PLoS ONE.* 2013;8(5):e63835.
12. Rousselle A, Sihn G, Rotteveel M, Bader M. (Pro)renin receptor and V-ATPase: from Drosophila to humans. *Clin Sci (Lond).* 2014;126(8):529-536.
13. Cruciat CM, Ohkawara B, Acebron SP, et al. Requirement of prorenin receptor and vacuolar H+-ATPase-mediated acidification for Wnt signaling. *Science.* 2010;327(5964):459-463.
14. Buechling T, Bartscherer K, Ohkawara B, et al. Wnt/Frizzled signaling requires dPRR, the Drosophila homolog of the prorenin receptor. *Curr Biol.* 2010;20(14):1263-1268.
15. Hermle T, Saltukoglu D, Grünewald J, Walz G, Simons M. Regulation of Frizzled-dependent planar polarity signaling by a V-ATPase subunit. *Curr Biol.* 2010;20(14):1269-1276.
16. Xu Y, Banerjee D, Huelsken J, Birchmeier W, Sen JM. Deletion of beta-catenin impairs T cell development. *Nat Immunol.* 2003;4(12):1177-1182.
17. Jeannet G, Scheller M, Scarpellino L, et al. Long-term, multilineage hematopoiesis occurs in the combined absence of beta-catenin and gamma-catenin. *Blood.* 2008;111(1):142-149.
18. Koch U, Wilson A, Cobas M, Kemler R, Macdonald HR, Radtke F. Simultaneous loss of beta- and gamma-catenin does not perturb hematopoiesis or lymphopoiesis. *Blood.* 2008;111(1):160-164.
19. Narumi K, Hirose T, Sato E, et al. Functional (pro)renin receptor is expressed in human lymphocytes and monocytes. *Am J Physiol Renal Physiol.* 2015;308(5):F487-F499.
20. Gray DH, Seach N, Ueno T, et al. Developmental kinetics, turnover, and stimulatory capacity of thymic epithelial cells. *Blood.* 2006;108(12):3777-3785.

ONLINE SUPPLEMENTAL DATA

New role for the (pro)renin receptor in T cell development

Geisberger *et al.*

Contains:

Supplemental Figures 1 - 6

Full experimental procedures

Supplemental references

Fig S1

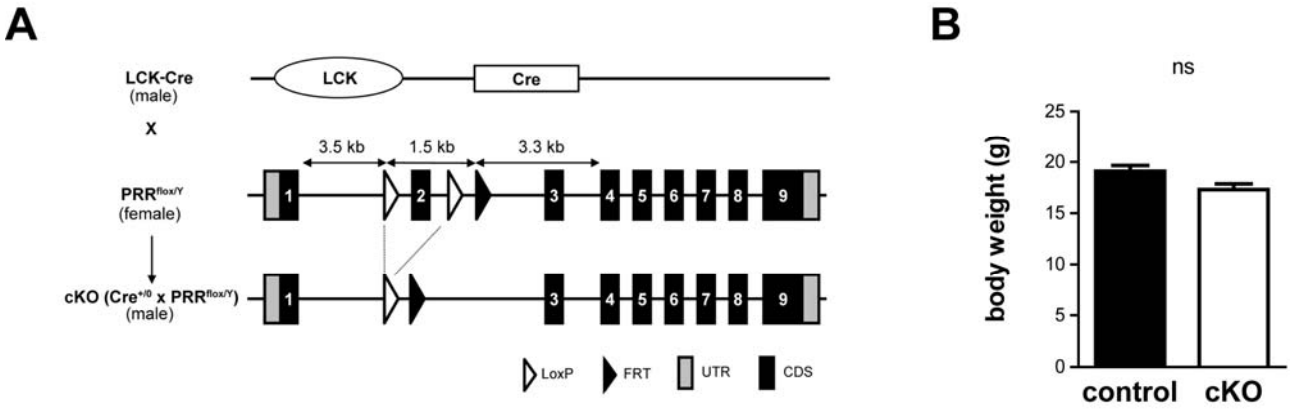

Supplemental Figure 1. Schematic of study.

A) Female mice carrying the loxP-flanked target allele encoding PRR were bred to Lck-cre transgenic male mice. As PRR is located on the X chromosome, first-generation knockout male offspring with PRR specific deleted in T cells *(ATP6AP2$^{flox/y}$;Lck-Cre)*.

B) Body weight between control and cKO mice was unchanged. N=20 (control); 9 (cKO).

Fig S2

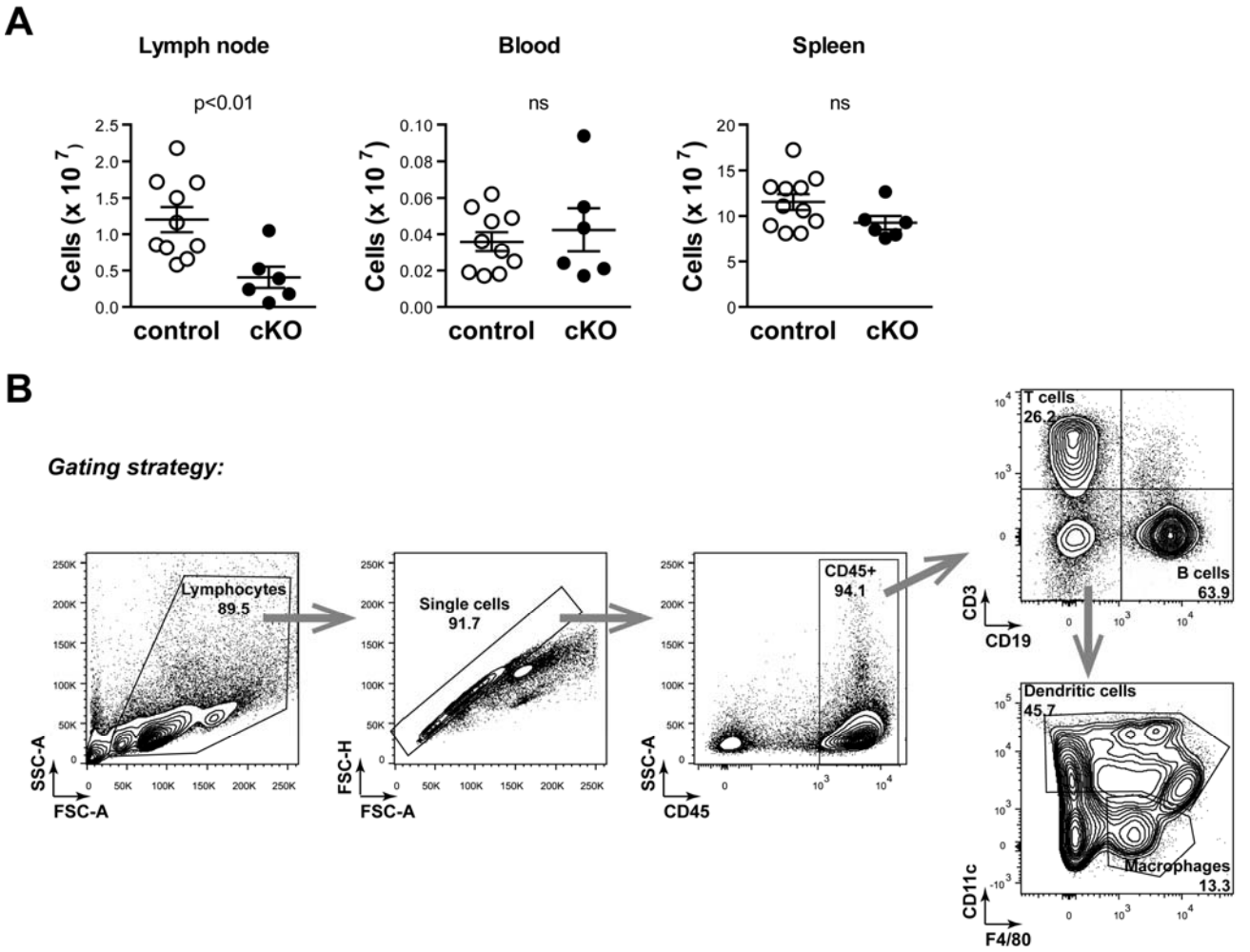
A
Lymph node
p<0.01
Cells (x 10 7)
control
cKO
Blood
ns
Spleen
ns
B
Gating strategy:
Lymphocytes
89.5
SSC-A
FSC-A
Single cells
91.7
FSC-H
CD45+
94.1
CD45
T cells
26.2
B cells
63.9
CD3
CD19
Dendritic cells
45.7
Macrophages
13.3
CD11c
F4/80

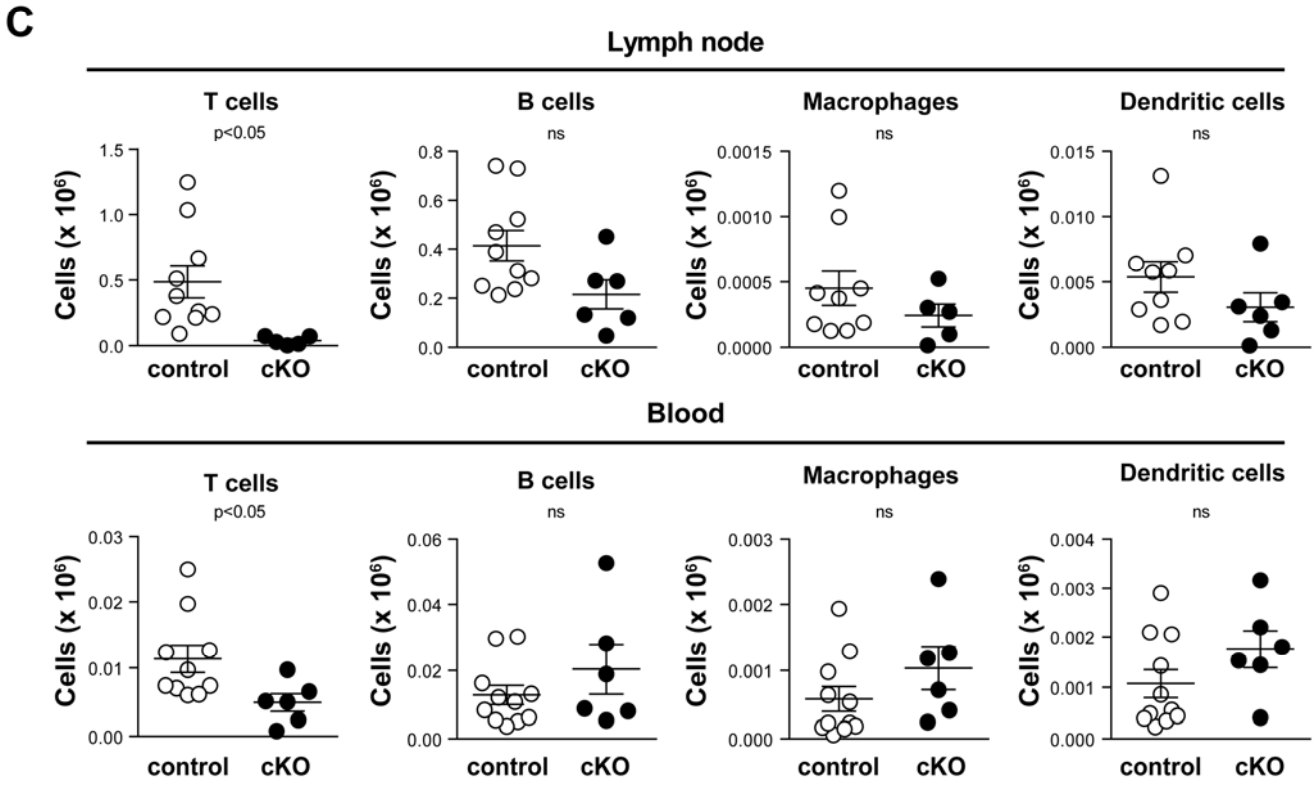
C
Lymph node
T cells
p<0.05
B cells
ns
Macrophages
ns
Dendritic cells
ns
Cells (x 10⁶)
control
cKO
Blood
T cells
p<0.05
B cells
ns
Macrophages
ns
Dendritic cells
ns

Supplemental Figure 2.Cellularity of peripheral lymph and circulating lymphocytes.

A) The cellularity of peripheral lymphoid organs (spleen and pooled lymph nodes) and PBMC's was determined in control and cKO mice. A significant decrease in the cellularity of lymph nodes was observed.

B) Gating strategy for flow cytometry analysis of the proportion of T, B, macrophages and dendritic cells (Fig 1A). Single celled lymphocytes were first gated as $CD45^+$, and then for CD3, CD19, CD11c and F4/80 expression.

C) The actual number of T cells ($CD3^+$), B cells ($CD19^+$), macrophages ($CD3^-CD19^-CD11c^-F4/80^+$) and dendritic cells ($CD3^-CD19^-CD11c^+$) was determined in lymph nodes and PBMC's from 7-8 week old control and cKO mice.

Fig S3

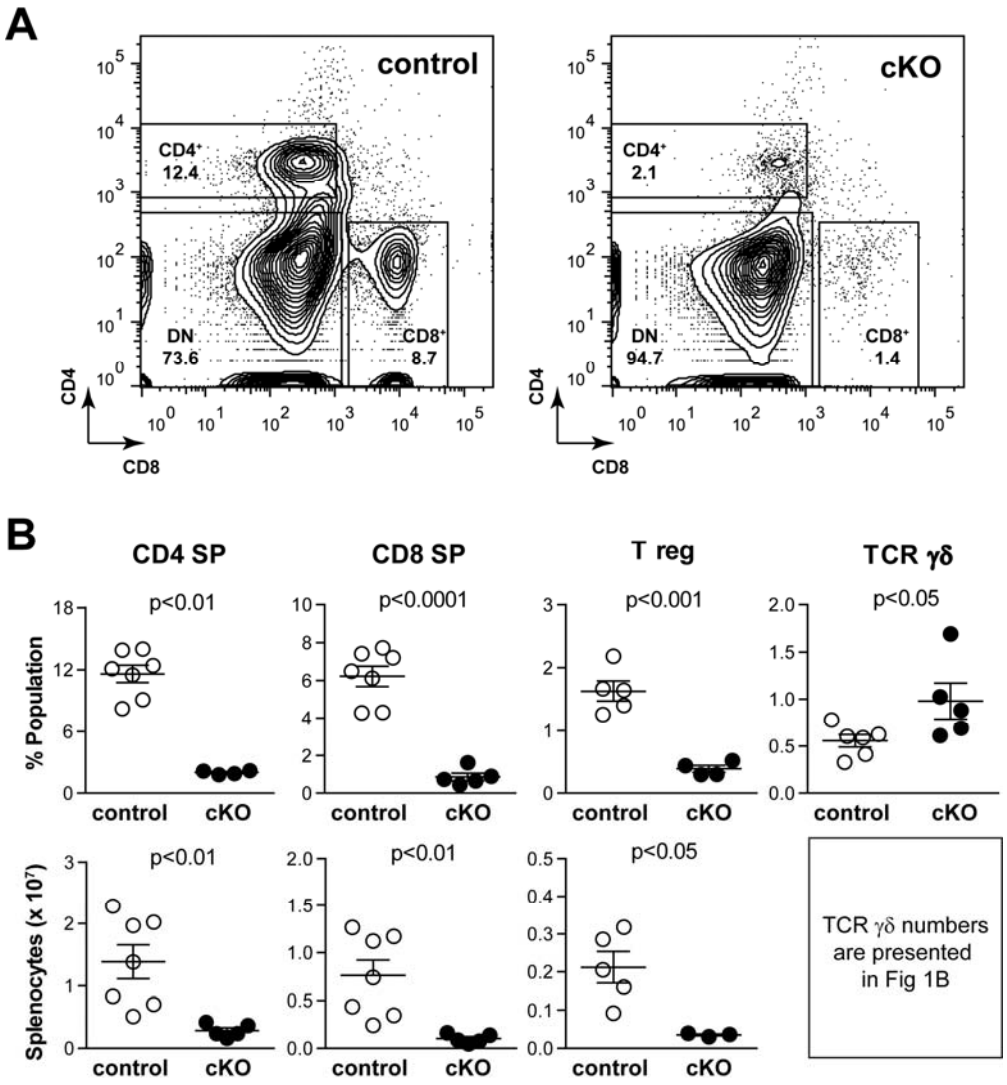

Supplemental Figure 3. Reduction in peripheral T cells.

A) Representative CD4 and CD8 expression in spleens of 6-8 week old control and cKO mice by flow cytometry.

B) The frequency (top row) and actual number (bottom row) of cell populations from **B**.

.

Fig S4

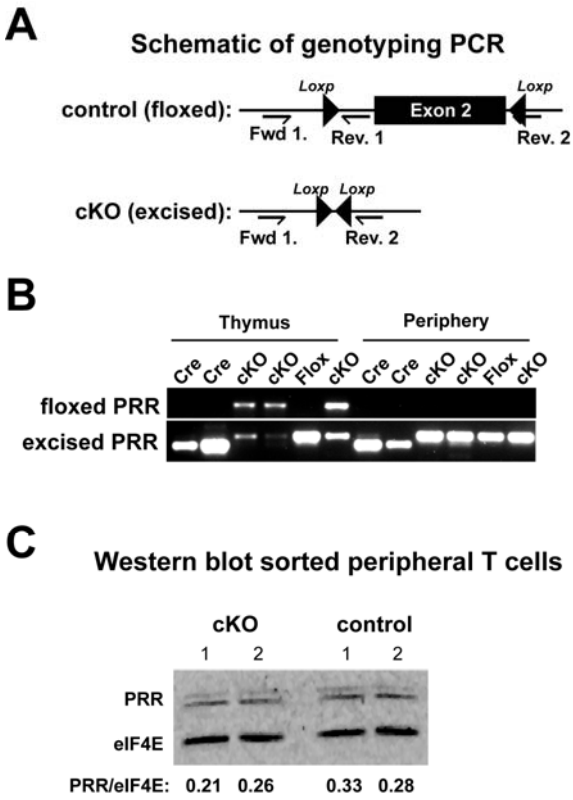

Supplemental Figure 4. Remaining peripheral T cells in cKO mice express normal levels of PRR.

A) Schematic for PCR's to detect the unexcised PRR gene ("floxed") and mutated/deleted gene in cKO ("excised").

B) From the same mouse, thymocytes (sorted DN4 cells) and peripheral T cells ($CD90.2^+$ MACS-enriched splenic T cells) were subjected to the PCR as in **A.** Six biological replicates are shown, where "Cre" and "Flox" corresponds to control mice, and "cKO" indicates PRR cKO mice.

C) PRR expression in sorted peripheral (pooled spleen and lymph node) $CD90.2^+$ T cells. Loading control eIF4E is shown.

Fig S5

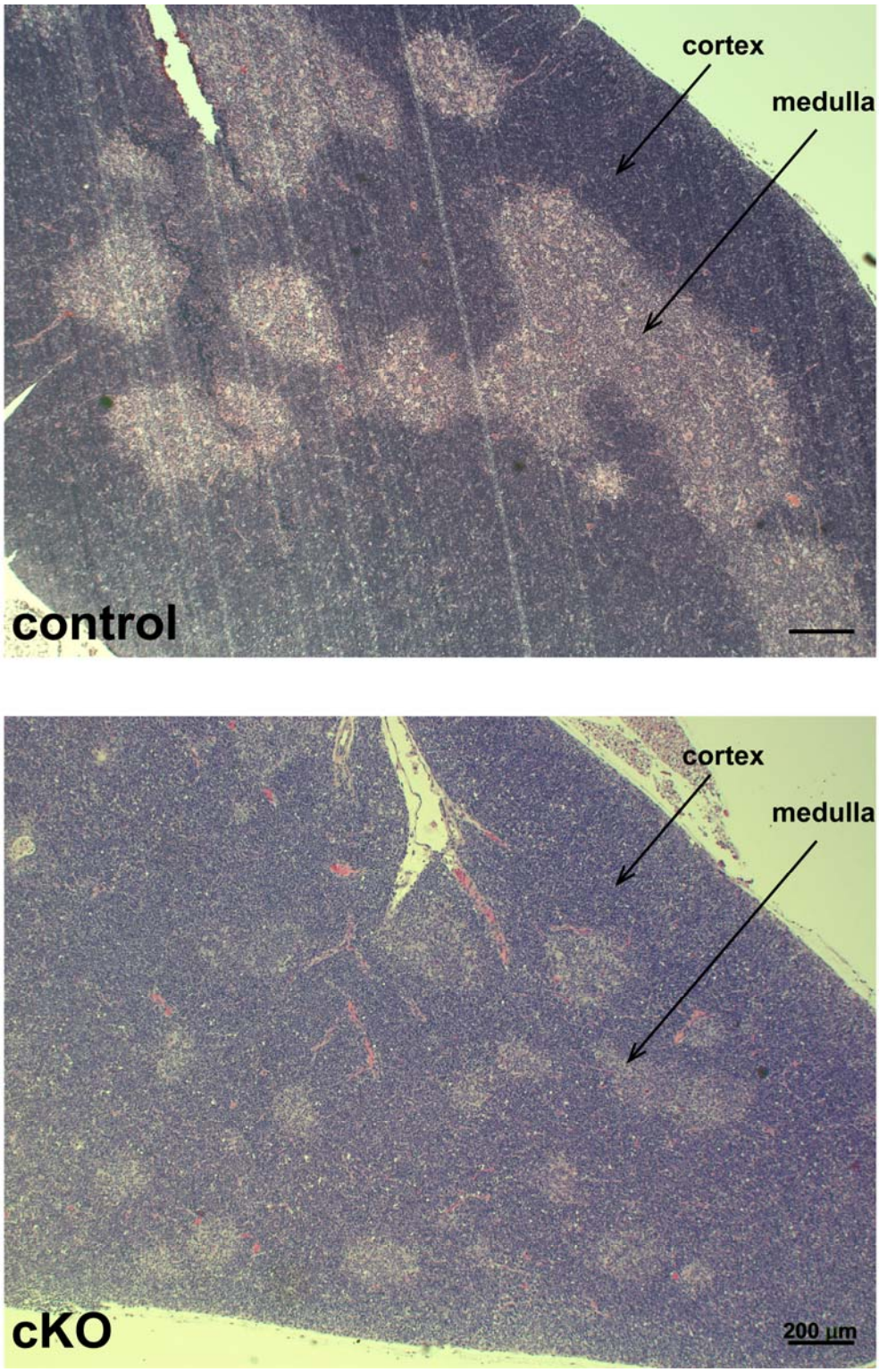

Supplemental Figure 5. Histological analysis of control and cKO thymii. Thymic architecture of control and cKO mice was determined by staining thymi with haeomotoxylin and eosin. A reduction in thymic medulla of cKO mice is observed; a characteristic secondary effect due to a lack of epithelial cell interaction with single positive T cells. Scale bars, 200 µm

Fig S6

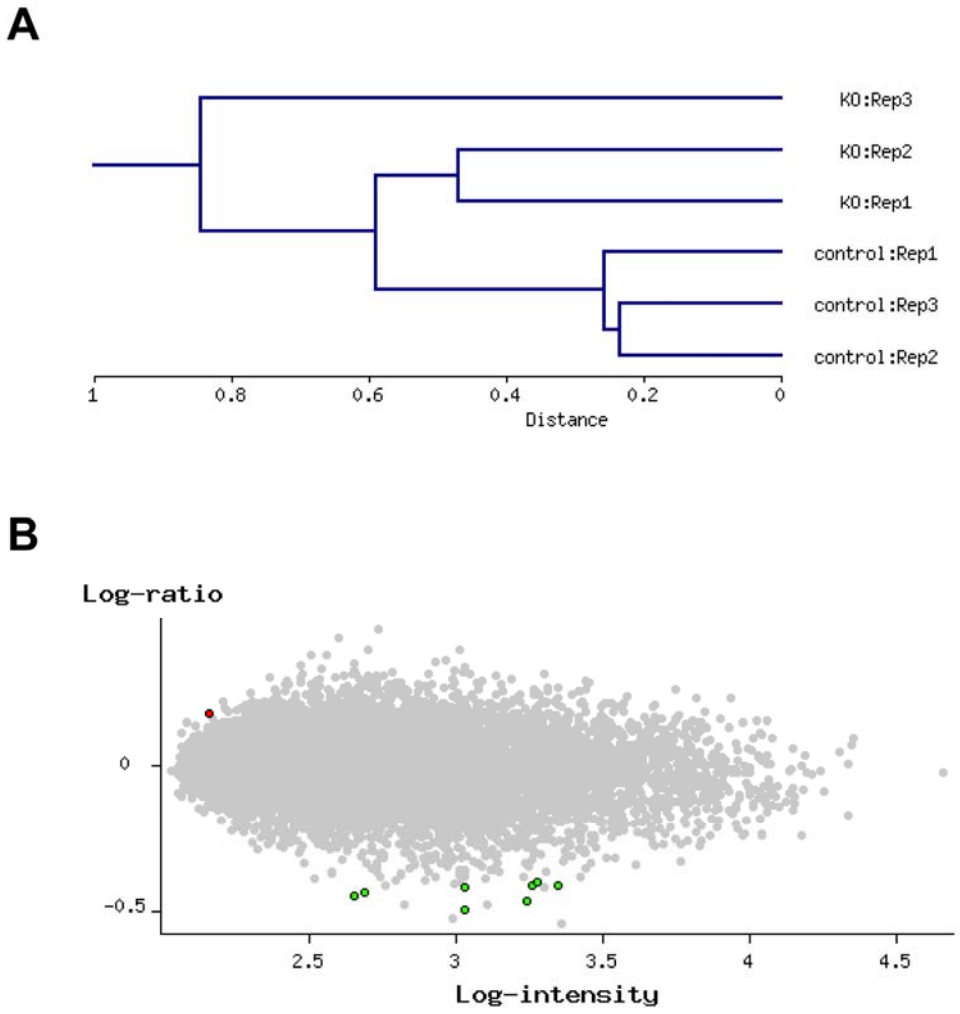

Supplemental Figure 6. Microarray quality control and ANOVA

A) Hierarchical clustering of averages of biological replicates (NIA array tool). N=3 control, N=3 cKO.

B) Differential gene expression between control and cKO samples, genes plotted as log-ratio versus log-intensity. Genes which significantly differentially regulated were identified by ANOVA (FDR<0.0.5). Genes that were significantly down-regulated are in green, up-regulated in red.

Full experimental procedures

Mice.

We generated mice with a conditional deletion of PRR from T cells by breeding female C57Bl/6 mice with loxP sites flanking exon 2 of the ATP6AP2 genes with male mice expressing Cre recombinase under the distal Lck promoter (founder line 3779)[1]. In this model, Cre is expressed specifically in early T cell development, beginning at the DN3 stage (**Fig S1A**). It has previously been reported that in this model no Cre is expressed at DN2, ~20-40% at DN3, and 90-100% at the DP stage[2]. As gamma-delta T cell receptor recombination begins at the DN2 stage of T cell development, alpha-beta T cell development is predominantly affected in this Lck-Cre model. Also, as PRR is located on the X chromosome, first-generation male offspring with PRR conditionally deleted in T cells were generated ($PRR^{flox/y}$;Lck-$Cre^{+/-}$) and are henceforth referred to as "cKO". Littermate control males ($PRR^{flox/y}$ or Lck-$Cre^{+/-}$) were pooled. Animal experiments were approved by the local authorities (LaGeSo, Berlin, Germany). Mice had normal weight (**Fig S1B**) and appeared healthy. They were housed under standard SPF-conditions and monitored daily to minimize harm.

Preparation of single-cell suspensions for flow cytometry.

Spleens and lymph nodes (two axial and two inguinal, pooled) were dissected from 7-8 week-old control and cKO mice. Thymuses were from 6 week-old mice, unless indicated otherwise. Organs were disrupted with forceps and scissors, and then passed through a 70 μM cell strainer (BD Bioscience) to generate single-cell suspensions. Peripheral blood mononuclear cells (PBMC's) were isolated by centrifugation through a Ficoll cushion (Ficoll-Paque PLUS, GE Healthcare). All samples were kept on ice. Red blood cells were removed from all single-cell suspensions by osmotic lysis. Lymphocytes were washed into FACS buffer (PBS with 0.5% (v/v) fetal calf serum (FCS) (S0615, Biochrom), and 2 mM EDTA). Cells were stained with trypan blue and the number of live cells was counted using a haemocytometer. For intracellular staining, cells

were first permeabilized using the CytoFix/CytoPerm Solution Kit (BD Bioscience), according to the manufacturer's protocol. For the staining of extracellular surface molecules, cells were resuspended into FACS buffer with the desired fluorescently labelled antibodies. Antibodies used were: CD3-APC-Cy7 (BD Biosciences, 557596), CD3-APC-eFluor660 (eBiosciences, 50-0032-82), CD4-FITC (BD Biosciences, 553729), CD4-PacificBlue (BD Biosciences 558107), CD8-PerCP-Cy5.5 (eBiosciences, 45-0081-82), CD8-eFluor450 (eBiosciences, 48-0081-82), CD8-PE (BD Biosciences, 553032), CD11c-Alexa647 (own polyclonal), CD19-PE (BD Biosciences, 12-0193-81), CD25-PE (BD Biosciences 553866), CD44-APC (eBiosciences, 17-0441-81), CD44-FITC (BD Biosciences, 561859), CD45-FITC (BD Biosciences, 553079), CD62L-APC (BD Biosciences, 561919), CD90.2-APC (BD Biosciences, 553007), F4/80-PacificBlue (eBiosciences, 48-4801), FOXP3-PerCP-Cy5.5 (eBiosciences, 75-5775-80), TCRβ (eBiosciences, 48-5961-82), TCRγδ-PE (BD Biosciences, 553178). After staining, cells were analysed on a BD FACS Canto II (BD Biosciences), and data was analyzed with the FlowJo software version 10 (Tree Star). Cell doublets were excluded by analysis of FSC-H vs FSC-A. Cell populations are expressed as a percentage of the respective organ, and the absolute number was also determined by multiplying by the total cell number of each organ. Cell populations were defined by the following gating strategies:

Peripheral organs (spleen, lymph nodes or PBMC's)	
(Pan) T cells	$CD45^+$ $CD3^+$
B cells	$CD45^+$ $CD19^+$
Macrophages	$CD45^+$ $CD3^-$ $CD19^-$ $CD11c^-$ $F4/80^+$
Dendritic cells	$CD45^+$ $CD3^-$ $CD19^-$ $CD11c^+$
$CD4^+$	$CD3^+$ $CD4^+$ $CD8^-$
$CD8^+$	$CD3^+$ $CD4^-$ $CD8^+$
TCRγδ	$CD3^+$ $CD4^-$ $CD8^-$ $TCR\gamma\delta^+$
T regulatory	$CD3^+$ $CD4^+$ $CD25^{hi}$ $icFOXP3^+$

Naïve ($CD4^+$ or $CD8^+$)	$CD44^{lo}$ $CD62L^+$
Thymus	
$CD4^+$ single positive	$CD4^+$ $CD8^-$ $CD25^-$ $CD44^-$
$CD8^+$ single positive	$CD4^-$ $CD8^+$ $CD25^-$ $CD44^-$
T regulatory	$CD3^+$ $CD4^+$ $CD25^{hi}$ $icFOXP3^+$
TCRγδ	$CD3^+$ $CD4^-$ $CD8^-$ $TCR\gamma\delta^+$
Double positive (DP)	$CD4^+$ $CD8^+$ $CD25^-$ $CD44^-$
Double negative (DN)	$CD4^-$ $CD8^-$ $CD25^-$ $CD44^-$
Intermediate single positive (ISP)	$CD4^-$ $CD8^+$ $CD25^-$ $CD44^-$
DN1	$CD4^-$ $CD8^-$ $CD25^-$ $CD44^+$
DN2	$CD4^-$ $CD8^-$ $CD25^+$ $CD44^+$
DN3	$CD4^-$ $CD8^-$ $CD25^+$ $CD44^-$
DN4	$CD4^-$ $CD8^-$ $CD25^-$ $CD44^-$

Enrichment of CD90.2 peripheral T cells (MACS).

Single cell suspensions were prepared from pooled lymph nodes and spleens as above. CD90.2+ T cells were enriched by positive selection with CD90.2 microbeads, according to the manufacturer's directions (Miltenyi Biotec, 130-049-101). MACS-enriched samples were stained with CD3 antibodies and analysed by flow cytometry. All samples had T cell purities of >91%.

Flow-assisted cell sorting (FACS).

Single cell suspensions were prepared from thymic tissue and peripheral organs as above. After staining with the desired antibodies, cells were sorted on a FACSAria (BD Biosciences). To sort, doublets were first excluded by FSC-A vs. FSC-H analysis, and then gated as desired. Sorted samples were re-analysed and all had 96-99% purity.

In vitro thymocyte survival assay.

The survival of control and cKO thymocytes was measured as published previously[3]. Briefly, single-cell suspensions of thymocytes from 3-week old mice were prepared as before, and 1 x 10^5 cells were cultured in RPMI with 10% FCS, 55 μM β-mercaptoethanol, 1%P/S and 10 ng/μL IL-7 (R&D Sytems). At the desired time points, the proportion of live cells was determined by staining with a Live/Dead Fixable Near IR stain (Life Technologies), as per the manufacturer's directions.

PCR.

T cell populations were isolated by FACS-sorting as described above. Genomic DNA was extracted from FACS-sorted cells by phenol/ethanol according to the protocol of Hansmann *et al* [4]. The analysis of TCRβ gene rearrangements was performed in DN4 sorted cells (>98% purity) according to the protocol of Hoshii *et al* [5].The analysis of the excision of the PRR gene was from various sorted thymic and peripheral T cell populations, all with a purity >95%. For detection of the PRR floxed gene (i.e. non-excised), DNA samples were incubated with the forward primer #1 (5'-AGCACTCTCTTCCAGGTATGTTGTG-3'), and reverse primer #1 (5'-CTGGATCCCGGAGCATGGGTAAAGG-3'). This resulted in the production of a 330 bp product for the floxed gene, or a 280 bp product for non-floxed/wildtype genes. For detection of the mutated gene after Cre-recombination "cKO" (i.e. excised), DNA samples were incubated with the forward primer #1 and reverse primer #2 (5'-GCCCCTCTCTTACAGTTCTATCAGT-3'). This PCR product was 326 bp in size. Primers for detection of the Cre recombinase were as described previously [6]. Bands were resolved on an agorose gel, and visualised with Ethidium bromide under ultra-violet light. Quantitative RT-PCR of Tcra rearrangement of gemonic sorted DP samples was performed as described previously[3].

Western blotting.

Single cell thymocyte suspensions were stained with anti-CD90.2 and sorted by FACS as above. The purity of $CD90.2^+$ cells was >95%. Sorted cells were then washed once with cold PBS and lyzed in RIPA buffer (#9806S, Cell Signaling) containing protease inhibitors. Total protein was determined by a Bradford assay and an equal amount of total protein was loaded per lane of a 15% SDS-PAGE. Proteins were blotted onto nitrocellulose membrane, blocked with 5% BSA and incubated with antibodies against PRR (Sigma) and eIF4E (Cell signaling) overnight at 4ºC. Blots were then incubated with infrared labelled secondary antibodies and bands visualised with an Odyssey system (Li-COR Biotechnology). Quantification of bands was performed with the program ImageJ [7].

Haemotoxylin and Eosin staining of thymii

Thymi were isolated from 6-week old control and PRR cKO mice. After fixing and embedding in paraffin, thymi were sectioned to a thickness of 8 μm for further analysis. Hematoxylin and eosin staining was performed by routine procedures. Sections were analyzed with a Zeiss Axioplan 2 imaging microscope (Carl Zeiss) at 5X magnification

.*Isolation of total RNA and real-time qPCR.*

FACS isolated DN3 cells (>96% purity) were washed once with PBS and then resuspended in Qiazol for the isolation of total RNA using an RNeasy RNA isolation kit (Qiagen), according to the manufacturer's protocol. The synthesis of cDNA and quantitative analysis of mRNA expressions by real-time PCR was performed as described previously[8]. Real-Time PCR was performed on a 7500 Fast Real-Time PCR System using TaqMan Fast Universal PCR Master Mix (both Applied Biosystems). Data were evaluated with the 7500 Fast System Software (Applied Biosystems). Samples were measured in triplicate and normalized against 18s. The primer and oligonucleotides for real-time PCR were designed using Primer Express®ABI PRISM software to

be species specific (except for the eukaryotic18s primer and probe) and exon overlapping. 18s (fw 5´ACATCCAAGGAAGGCAGCAG 3´, rev 5´ TTTTCGTCACTACCTCCCCG 3´, probe 5´ FAM-CGCGCAAATTACCCACTCCCGAC-TAMRA 3´); mouse PRR (fw 5' CCAGTTTGTTGTCTCGTCATAAGC 3', rev 5' ACCTGCCAGCTCCAATGAAT 3', probe 5' FAM-TCTAGCCAAGGACCATTCACCCGACTT-TAMRA 3').

Microarray.

Total RNA was isolated from FACS-sorted DN3 cells as above. Due to the low RNA content in these samples, amplified cDNA was prepared with the Ovation PicoSL WTA System V2 (NuGEN Technologies, CA, USA) according to the manufacturer's directions. Three μg of amplified and purified cDNA was then labelled with biotin by the Encore BiotinIL Module (also NuGEN), according to the manufacturer's directions. Finally, 900 ng of labelled target was analyzed using the Illumina Mouse ref 8v2.0 array. Microarray data are available in the ArrayExpress database (www.ebi.ac.uk/arrayexpress) under accession number E-MTAB-12345. Data was processed on the Illumina GenomeStudio V2011.1 Platform (Gene Expression Module 1.9.0), quantile normalized on a probe level, without background correction (Table S1A). The data was then analyzed with the NIA Array Analysis tools (http://lgsun.grc.nia.nih.gov/ANOVA/index.html). First, hierarchical clustering of averages was performed for assessment of the quality of biological replicates **(Fig S6A)**. Genes which were significantly differentially regulated were identified by ANOVA–false discovery rate (FDR) statistics (http://lgsun.grc.nia.nih.gov/ANOVA) (FDR<0.05; **Fig S6B**). Fold-changes were calculated from mean expression values in control to cKO samples. A list containing 1133 genes were identified as having a difference in expression >1.5-fold. This list was then analyzed for the enrichment of gene ontology (GO) pathways with the online tool DAVID (http://david.abcc.ncifcrf.gov/) (Table S1B). Due to the high overlap of gene names within these pathway lists, for presentation purposes only 10 representative GO pathways are shown. Full details are provided in Table S1B.

Statistics.

All data is presented as mean ± standard error. Outliers were first excluded using a Grubbs' statistical test. Normality of data was assessed according to the Kolmogorov-Smirnov test, and then analyzed by either two-sided Student's t-tests (parametric) or a Mann-Whitney U-tests (for non-parametric data). Analysis of *Tcra* rearrangement in DP cells, and thynmocyte survival over time was by ordinary two-way ANOVA with Sidak's multiple comparison test.

Supplemental references

1. Zhang DJ, Wang Q, Wei J, et al. Selective expression of the Cre recombinase in late-stage thymocytes using the distal promoter of the Lck gene. *J Immunol*. 2005;174(11):6725-6731. Prepublished on 2005/05/21 as DOI.

2. Shi J, Petrie HT. Activation kinetics and off-target effects of thymus-initiated cre transgenes. *PLoS One*. 2012;7(10):e46590. Prepublished on 2012/10/11 as DOI 10.1371/journal.pone.0046590.

3. Hao B, Naik AK, Watanabe A, et al. An anti-silencer- and SATB1-dependent chromatin hub regulates Rag1 and Rag2 gene expression during thymocyte development. *J Exp Med*. 2015;212(5):809-824. Prepublished on 2015/04/08 as DOI 10.1084/jem.20142207.

4. Hansmann L, Schmidl C, Boeld TJ, et al. Isolation of intact genomic DNA from FOXP3-sorted human regulatory T cells for epigenetic analyses. *Eur J Immunol*. 2010;40(5):1510-1512. Prepublished on 2010/03/05 as DOI 10.1002/eji.200940154.

5. Hoshii T, Kasada A, Hatakeyama T, et al. Loss of mTOR complex 1 induces developmental blockage in early T-lymphopoiesis and eradicates T-cell acute lymphoblastic leukemia cells. *Proc Natl Acad Sci U S A*. 2014;111(10):3805-3810. Prepublished on 2014/02/26 as DOI 10.1073/pnas.1320265111.

6. Riediger F, Quack I, Qadri F, et al. Prorenin Receptor Is Essential for Podocyte Autophagy and Survival. *J Am Soc Nephrol*. 2011. Prepublished on 2011/10/29 as DOI 10.1681/ASN.2011020200.

7. Schneider CA, Rasband WS, Eliceiri KW. NIH Image to ImageJ: 25 years of image analysis. *Nat Methods*. 2012;9(7):671-675. Prepublished on 2012/08/30 as DOI.

8. Marko L, Henke N, Park JK, et al. Bcl10 mediates angiotensin II-induced cardiac damage and electrical remodeling. *Hypertension*. 2014;64(5):1032-1039. Prepublished on 2014/09/04 as DOI 10.1161/HYPERTENSIONAHA.114.03900.